Growth hormone induces Notch1 signaling in podocytes and contributes to proteinuria in diabetic nephropathy

Received for publication, April 19, 2019, and in revised form, August 28, 2019 Published, Papers in Press, September 11, 2019, DOI 10.1074/jbc.RA119.008966

Rajkishor Nishad[‡], **Dhanunjay Mukhi**[‡], **Syed V. Tahaseen**[§], **Sathish Kumar Mungamuri**[¶], **and Anil K. Pasupulati**[‡1]

From the [‡]*Department of Biochemistry, School of Life Sciences, University of Hyderabad, Hyderabad, India 500046, the* [§]*Department of Biochemistry, SRR & CVR Degree College, Vijayawada, India 520010, and the* [¶]*Division of Food Safety, National Institute of Nutrition, Hyderabad, India 500007*

Edited by Jeffrey E. Pessin

Growth hormone (GH) plays a significant role in normal renal function and overactive GH signaling has been implicated in proteinuria in diabetes and acromegaly. Previous results have shown that the glomerular podocytes, which play an essential role in renal filtration, express the GH receptor, suggesting the direct action of GH on these cells. However, the exact mechanism and the downstream pathways by which excess GH leads to diabetic nephropathy is not established. In the present article, using immortalized human podocytes *in vitro* and a mouse model *in vivo*, we show that excess GH activates Notch1 signaling in a γ-secretase–dependent manner. Pharmacological inhibition of Notch1 by γ-secretase inhibitor DAPT (*N*-[*N*-(3,5-Difluorophenacetyl)-L-alanyl]-*S*-phenyl glycine *t*-butylester) abrogates GH-induced epithelial to mesenchymal transition (EMT) and is associated with a reduction in podocyte loss. More importantly, our results show that DAPT treatment blocks cytokine release and prevents glomerular fibrosis, all of which are induced by excess GH. Furthermore, DAPT prevented glomerular basement membrane thickening and proteinuria induced by excess GH. Finally, using kidney biopsy sections from people with diabetic nephropathy, we show that Notch signaling is indeed up-regulated in such settings. All these results confirm that excess GH induces Notch1 signaling in podocytes, which contributes to proteinuria through EMT as well as renal fibrosis. Our studies highlight the potential application of γ-secretase inhibitors as a therapeutic target in people with diabetic nephropathy.

Renal interstitial fibrosis is the hallmark of progressive chronic kidney disease, which correlates well with renal failure (1). Renal fibrosis is characterized by myofibroblast proliferation and activation, epithelial cell dysfunction, leukocyte migration, excessive production, and deposition of extracellular matrix (2). In response to kidney damage, there will be infiltration of mature myofibroblasts from various sources including interstitial fibroblasts, pericytes, endothelial cells, and circulating fibrocytes (2). Previous studies have shown that multiple pathways such as the transforming growth factor-β (TGF-β)[2]/Smad2/3 and Notch signaling are involved in epithelial cell dysfunction and fibroblast activation, which leads to the progression of kidney fibrosis (2).

In the early glomerular development, particularly at the S-shaped body formation, podocyte fate determination is regulated by the highly conserved Notch signaling, which transduces short-range signals between neighboring cells (3–6). The Notch pathway comprises 4 transmembrane Notch receptors (Notch 1–4) and 5 Notch ligands (Delta-like 1, 3, and 4, and Jagged 1 and 2). After ligand binding, Notch receptors undergo a series of cleavages catalyzed by the ADAM proteases and γ-secretase complex, which results in the release of the Notch intracellular domain (NICD, Fig. S1); this process can be inhibited by the γ-secretase inhibitor and dibenzoazepine (7). The resulting NICD translocates into the nucleus (8), wherein it forms a ternary complex by associating with the DNA-binding protein, retinol-binding protein-jk and the coactivator, Mastermind-like protein 1 and activates expression of target genes (9–12).

Vooijs *et al.* (13) have reported that Notch1 is highly active in the developing kidney; however, in the mature kidney detection of active Notch1 is very little. Inhibition of Notch signaling during early development of the mouse kidney results in a severe deficiency of glomerular podocytes, indicating the importance of Notch signaling during kidney development (3). On the other hand, persistent activation of Notch signaling in the mature kidney leads to podocyte damage and subsequent kidney failure (14). Further studies had also shown that ectopic Notch activation in terminally differentiated podocytes is correlated with both diffuse mesangial sclerosis and focal segmental glomerulosclerosis, which are associated with *de novo* Pax2 expression and p53-induced podocyte apoptosis, respectively (14, 15). It was also observed that the genetic deletion of the

This work was supported by Science and Engineering Research Board Grant EMR/2015/2076 (to A. K. P.), Research Fellowships from the University Grants Commission, India (to R. N. and D. M.), and a Ramanujan Fellowship from Department of Science and Technology - Science and Engineering Research Board Grant (to S. K. M.). The authors declare that they have no conflicts of interest with the contents of this article.

This article contains Figs. S1–S5.

The microarray data reported in this paper have been submitted to the Gene Expression Omnibus (GEO) database under GEO accession no. GSE21327.

[1] To whom correspondence should be addressed. Tel.: 91-40-23134519; E-mail: pasupulati.anilkumar@gmail.com.

[2] The abbreviations used are: TGF-β, transforming growth factor β; NICD, Notch intracellular domain; GH, growth hormone; GBM, glomerular basement; EMT, epithelial to mesenchymal transition; qRT, quantitative RT; DAPT, *N*-[*N*-(3,5-difluorophenacetyl)-L-alanyl]-*S*-phenylglycine *t*-butyl ester; UACR, urinary albumin-creatinine ratio; GFR, glomerular filtration rate; DN, diabetic nephropathy; PAS, periodic acid-Schiff; TEM, transmission electron microscope; DAPI, 4′,6-diamidino-2-phenylindole; α-SMA, α-smooth muscle actin.

Notch pathway in tubular epithelial cells ameliorates renal fibrosis in the unilateral ureteral obstruction murine model and folic acid-induced renal fibrosis (16). These data reveal that Notch signaling plays an essential role in the fibrotic pathogenesis. However, the precise underlying cellular mechanisms are not fully understood.

Although many studies show that the role of Notch1 signaling in glomerular diseases (17–19), the correlation between activated Notch1 signaling and diabetic proteinuria remains to be elucidated. Elevated levels of circulating growth hormone (GH) are associated with the development of nephropathy in "type 1 diabetes" and "acromegaly" (20, 21). Conditions of elevated GH are typified by hyperfiltration, glomerulosclerosis, and albuminuria. On the other hand, both decreased GH secretion and action can protect from glomerular complications (22). Previously, we have established the role of GH on glomerular cells, particularly on podocytes (23, 24). Our present study demonstrates that excess GH activates Notch signaling in human podocytes as well as in the murine kidneys. Blocking the activated Notch signaling through pharmacological inhibition of γ-secretase function reverted the excess GH-induced kidney fibrosis, interstitial infiltration of plasma-lymphocytic cells and proteinuria, hindered the glomerular basement membrane (GBM) thickening with severe foot process effacement in mice as well as epithelial to mesenchymal transition (EMT) and fibrotic marker expression of podocytes. Our present study demonstrates that an elevated level of circulatory GH after embryonic development may compromise the podocyte function by activation of Notch signaling and could represent a new pharmacological target.

Results

GH induces Notch1 activation in immortalized human podocytes

To identify the biochemical pathways downstream of GH signaling that are hyperactivated in podocytes in response to excess GH, we previously performed microarray analysis (GEO accession number GSE21327) on immortalized human podocytes treated with GH and identified transcriptional activation of EMT regulator "ZEB2" (24). By reanalyzing the same microarray data, we now identified that in response to GH treatment, Notch1 signaling is up-regulated in human podocytes (Fig. S2). To reconfirm the up-regulation of Notch signaling pathway by GH in podocytes, we also analyzed the expression of Notch1 and its targets Hes1 and Jag1 in nondiabetic mouse kidney ($n = 18$) *versus* diabetic nephropathy mouse kidney ($n = 21$) in the Hodgin diabetes mouse glomerulus data set available at Nephroseq (https://nephroseq.org),[3] which shows that diabetic nephropathy kidneys overexpress Notch1 and its target genes, *Hes1* and *Jag1* (Fig. 1*A*). Next, to validate the data obtained in our microarray analysis as well as that from Nephroseq, we measured the mRNA levels of both Notch1 and its target genes by quantitative RT (qRT)-PCR, and as expected, the levels of Notch1 (full-length) and its targets were up-regulated with GH treatment in the human podocytes (Fig. 1*B*). GH had induced the expression of activated Notch1 (NICD1) and its target proteins in both concentration (Fig. 1*C*) and time-dependent (Fig. 1*D*) manners. γ-Secretase is an intramembrane protease that cleaves many membrane proteins including Notch1, which generates the NICD1 (25). Accordingly, we also observed a time-dependent increase in γ-secretase activity with GH treatment in human podocytes (Fig. 1*E*). All these data suggests that Notch1 signaling is up-regulated in response to GH treatment in human podocytes.

γ-Secretase activity is required for GH-mediated Notch activation

To confirm the role of γ-secretase in GH-induced Notch1 activation, we next treated the human podocytes with GH in the absence or presence of well-established γ-secretase inhibitor, DAPT (*N*-[*N*-(3,5-difluorophenacetyl)-L-alanyl]-*S*-phenylglycine *t*-butyl ester). As expected, DAPT treatment to the GH-exposed human podocytes has decreased the γ-secretase activity in a time-dependent manner (Fig. 2*A*). GH was not able to induce the expression of Notch1 or its target genes (*Hes1* and *Hey1*) in the presence of DAPT in human podocytes as measured by qRT-PCR (Fig. 2*B*), Western blotting (Fig. 2*C*), and immunofluorescence (Fig. 2*D*). Furthermore, we continued our quest of understanding the effect of GH on Notch signaling *in vivo*. Similar to the observations *in vitro*, GH treatment led to the induction of NICD1, Jag1, and NICD targets: Hes1 and Hey1 in glomerular sections from mice as measured with immunostaining (Fig. 3, *A–D*) and Western blotting (Fig. 3, *E* and *F*). DAPT inhibited NICD1 accumulation and induction of its targets in glomerular sections (Fig. 3, *A*, *C*, and *D*), glomerular lysates (Fig. 3*E*), and primary podocytes (Fig. 3*F*) isolated from GH-treated mice. However, the expression of Jag1 was unaffected by DAPT treatment (Fig. 3, *B*, *E*, and *F*). It should be noted that the data from isolated podocytes corroborate with that from glomerular lysate (Fig. 3, *E* and *F*). Together, the data confirm that GH stimulates NICD1 expression in glomeruli and podocytes, and functional γ-secretase is required to activate GH-dependent Notch1 signaling.

Activated Notch signaling is required for GH-induced EMT in podocytes

Previously, we established that excess GH elicits EMT in podocytes (24). Thus, we analyzed the influence of Notch signaling in GH-induced EMT in podocytes. GH treatment induced the EMT markers (E-Cad, N-Cad, Snail, Slug, ZEB2, Vimentin, and α-SMA) in human podocytes and mouse glomerulus as shown at both mRNA (Fig. 4*A*) and protein levels (Fig. 4, *B* and *C*). DAPT treatment abrogated this effect of GH in human podocytes (Fig. 4, *A* and *B*) and mouse glomerulus (Fig. 4*C*).

Remodeling of actin filaments is necessary for EMT (26). To confirm the physiological function of EMT induced by GH, we next performed the phalloidin staining of the podocytes treated with GH, with or without DAPT treatment. The results presented in Fig. 4*D* suggests that there is complete disorganization of the actin filaments in the podocytes treated with GH, and can be rescued by co-treatment with DAPT (Fig. 4*D*). Quantification of F-actin stress fiber distribution revealed a sig-

[3] Please note that the JBC is not responsible for the long-term archiving and maintenance of this site or any other third party hosted site.

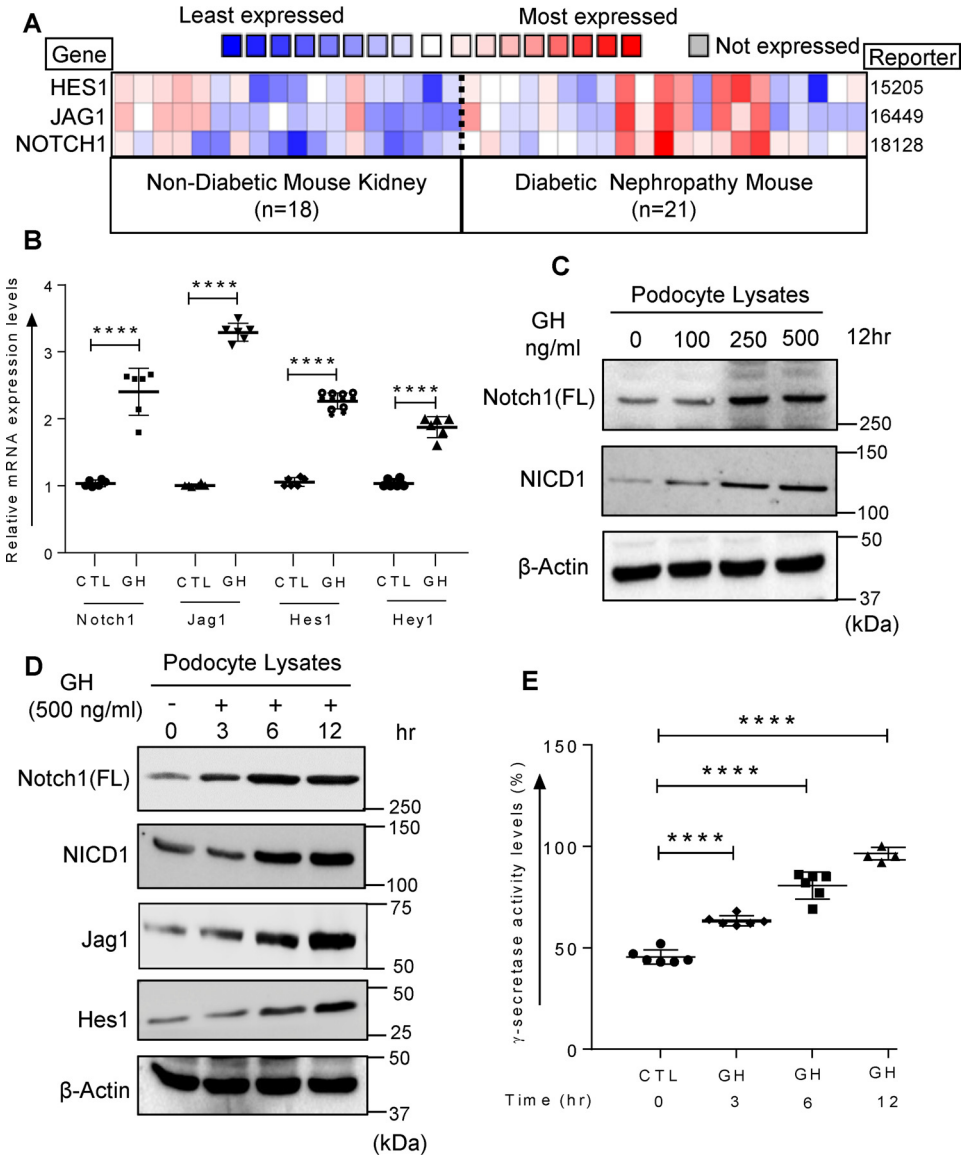

Figure 1. GH induces Notch1 activation in immortalized human podocytes. *A*, Nephroseq (University of Michigan O'Brien Renal Center, Michigan, Ann Arbor, MI) analysis comparing *HES1*, *JAG1*, and *NOTCH1* expression levels from nondiabetic mouse kidney ($n = 18$) *versus* diabetic nephropathy mouse kidney ($n = 21$) in Hodgin diabetes mouse glomerulus. Data indicate that expression of these genes increased >1.5-fold in the diabetic group. *B*, qRT-PCR analysis showing the expression of Notch pathway genes (*Notch1*, *Jag1*, *Hes1*, and *Hey1*) in human podocytes treated with GH (500 ng/ml) or without GH (*CTL*) for 30 min. mRNA levels were normalized to β-Actin levels and presented as fold-change on the *y* axis. ****, $p < 0.0001$. *C*, immunoblotting analysis showing the expression of Notch1 full-length (*FL*), active Notch1 (NICD1), and β-Actin in human podocytes treated with GH (100 to 500 ng/ml) for 12 h. *D*, immunoblotting analysis showing the expression of Notch1 (*FL*), NICD1, Jag1, Hes1, and β-Actin in human podocytes treated with GH (500 ng/ml) or the indicated time intervals (0 to 12 h). *E*, γ-secretase activity in human podocytes treated with or without GH (500 ng/ml) for 0–12 h. ****, $p < 0.0001$. Data represent the mean ± S.D. ($n = 6$) and statistical significance was analyzed by Student's *t* test.

nificant loss (60 ± 5%) of stress fibers in podocytes exposed to GH, whereas DAPT ameliorated GH-induced injury to the actin stress fibers (Fig. 4*E*).

Furthermore, to confirm the role of Notch1 signaling in GH-induced EMT in the podocytes, we also performed the cell migration assay. Although GH treatment alone to the podocytes completely covered the wound by 12 h, DAPT treatment abrogated this GH-induced phenotype (Fig. 4*F*). Quantification of wound coverage in response to CTL, GH, and GH + DAPT exposure, GH solely enhanced the migration of podocytes (90 ± 8%, Fig. 4*G*). All these results confirm that excess GH induces EMT in the podocytes and activated Notch signaling is essential for GH-induced EMT in podocytes.

Activated Notch signaling is required for GH-induced interstitial infiltration of plasma-lymphocytic cells and fibrosis in kidneys

Diabetes is characterized by mild, but significant glomerulosclerosis, and GH has been shown to contribute to the glomerulosclerosis (27). Next, we treated the mice with GH and prepared the paraffin-embedded kidney sections to look for interstitial infiltration of plasma-lymphocytic cells. As previously noted, our hematoxylin and eosin staining of the kidney sections showed interstitial infiltration of plasma-lymphocytic cells in mice treated with the GH (Fig. 5*A*). We also observed enhanced fibrosis in the mice kidneys treated with the GH, as analyzed by both periodic acid-Schiff (PAS) (Fig. 5*B*) and Mas-

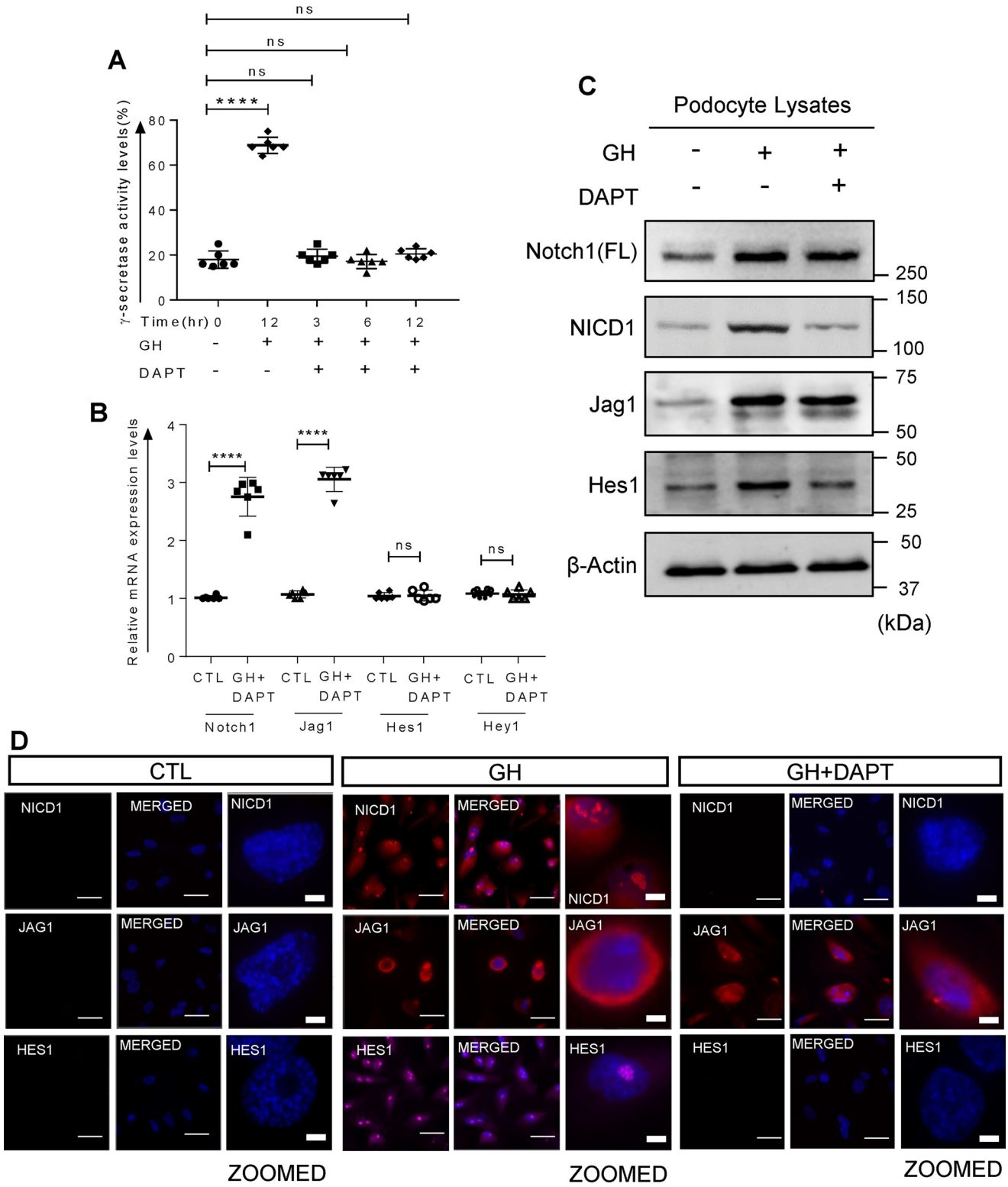

Figure 2. DAPT limits the hyperactive Notch signaling in human podocytes by inhibiting the γ-secretase activity. *A*, γ-secretase activity in human podocytes treated with GH or GH + DAPT for the indicated time intervals (3–12 h). ****, $p < 0.0001$, *ns*, not significant. *B*, qRT-PCR analysis showing the expression of *Notch1*, *Jag1*, *Hes1*, and *Hey1* in human podocytes treated with GH (500 ng/ml) + DAPT (5 μg/ml). β-Actin was used as an internal control. ****, $p < 0.0001$. *C*, immunoblotting analysis showing the expression of Notch1 (*FL*), NICD1, Jag1, and Hes1 in CTL, GH, and GH + DAPT-treated (12 h) human podocytes. *D*, immunofluorescence analysis for NICD1, Jag1, and Hes1 in CTL, GH, and GH + DAPT treated (12 h) human podocytes (×630). *Scale bar* = 20 μm. Data presented as mean ± S.D. ($n = 6$) and statistical significance was analyzed by Student's *t* test.

son's trichrome (Fig. S3*A*) stainings. Quantification of the Masson's trichrome-stained area revealed that GH enhanced glomerular fibrosis (50 ± 10%, Fig. S3*B*). These data also correlated with increased expression of cytokines (Fig. 5*C*) and fibrotic marker in GH-treated mice, as measured at both mRNA and protein (Fig. S3, *C* and *D*) levels.

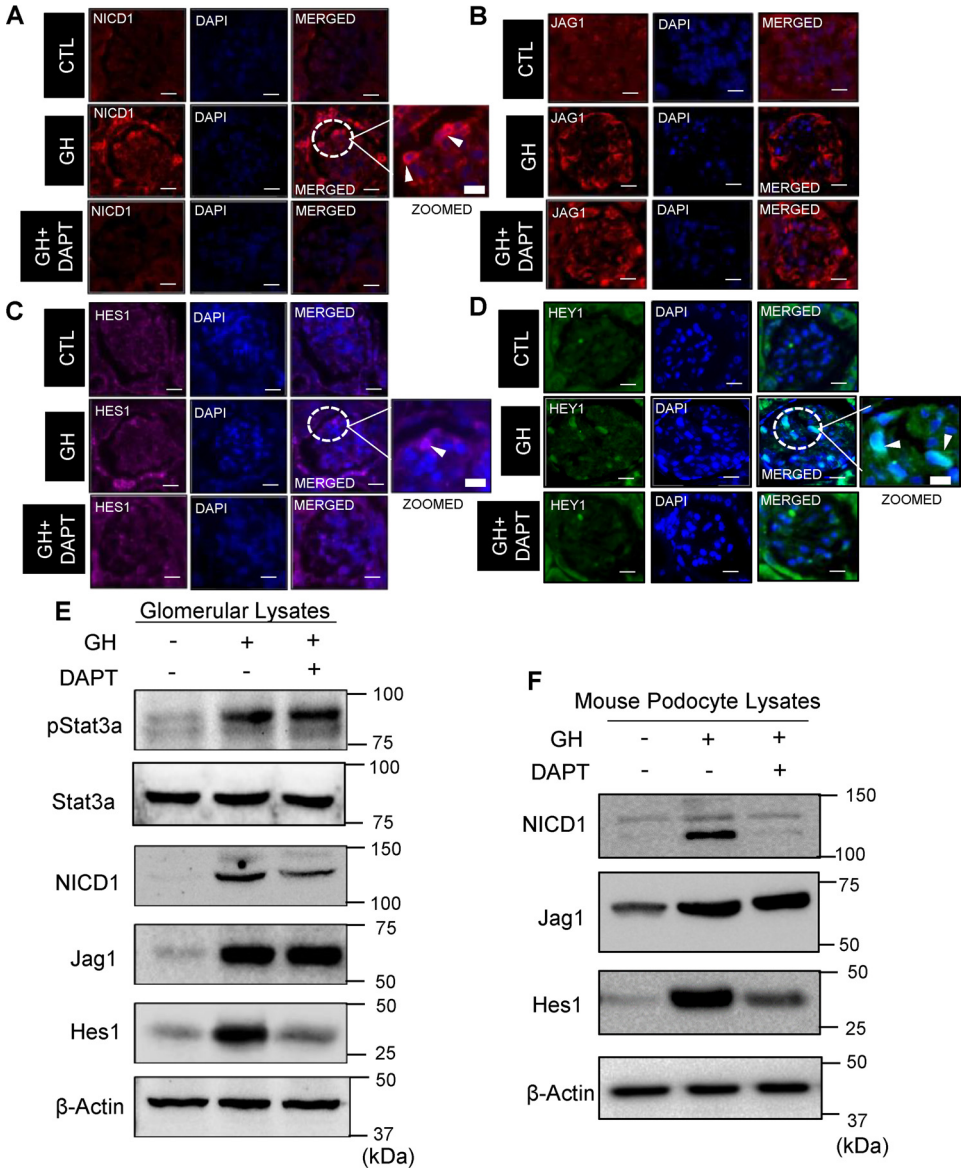

Figure 3. GH induces Notch signaling in glomerulus of mice kidney. *A–D*, representative images of immunostaining for NICD1 (*A*), Jag1 (*B*), Hes1 (*C*), and Hey1 (*D*) in glomeruli from CTL, GH, and GH + DAPT mice ($n = 6$). We employed DyLight 594-conjugated secondary antibody for NICD1 and Jag1; Cy5-conjugated secondary antibody for Hes1; and DyLight 488-conjugated secondary antibody for Hey1. These sections were counterstained with DAPI. *Scale bars* = 20 μm (×630). *E*, Western blot analysis showing the expression of pStat3a, total Stat3a, NICD1, Jag1, and Hes1 from CTL, GH, and GH + DAPT-treated mice glomerular lysates ($n = 6$). Expression of β-Actin was used as an internal control. *F*, Western blot analysis showing the expression of NICD1, Jag1, and Hes1 in primary mouse podocytes isolated from CTL, GH, and GH + DAPT- treated mice. Expression of β-Actin was used as an internal control. Data are presented as mean ± S.D. and statistical significance was calculated by using Student's *t* test.

Indeed, treatment of mice with DAPT had reversed the GH-induced nonresident cell infiltration into the kidneys (Fig. 5*A*) and was able to reverse the fibrosis as evidenced by periodic acid-Schiff (Fig. 5*B*) and Masson's trichrome (Fig. S3*A*) stainings. Mesangial expansion and glomerular damage score were found elevated with GH treatment (Fig. 5, *C* and *D*). DAPT treatment also inhibited the GH-induced cytokine and fibrotic gene induction (Fig. 5*E*); and reversed podocyte-specific marker genes expression as measured at both mRNA and protein levels (Fig. S3, *C* and *D*). To further evaluate whether the cytokines released from these podocytes are indeed functional, and DAPT blocked the function of these cytokines, we next performed classical chemotaxis assay using J774A.1 macrophages. As expected, the macrophages were able to fill the gap, when treated with conditioned medium collected from podocytes treated with the GH, whereas this function was completely blocked when similar conditioned medium from podocytes treated with GH + DAPT was used (Fig. S4*A*). The conditioned medium from the untreated podocytes was used as a control. Quantification of the wound coverage in response to CTL, GH, GH + DAPT, and C5a exposure, GH-treated spent medium solely enhanced the migration of J774A.1 macrophages (70 ± 10% increase, $p < 0.001$, Fig. S4*B*).

Kidney fibrosis leads to thickening of the GBM, which consequently results in podocyte foot process effacement (28). To confirm whether a similar phenomenon also happens in our GH-induced proteinuria mice model, we next performed transmission EM studies to analyze the structural changes in the

GBM as well as podocyte foot processes in mice kidney samples. Our results show that whereas GH treatment in the mice leads to GBM thickening and podocyte foot process effacement, similar treatment of GH along with DAPT completely abrogated this effect (Fig. 5, *F* and *G*). All these results confirm that excess GH activates Notch1 signaling, which in turn leads to infiltration of circulating cells in the kidneys and leading to its fibrosis.

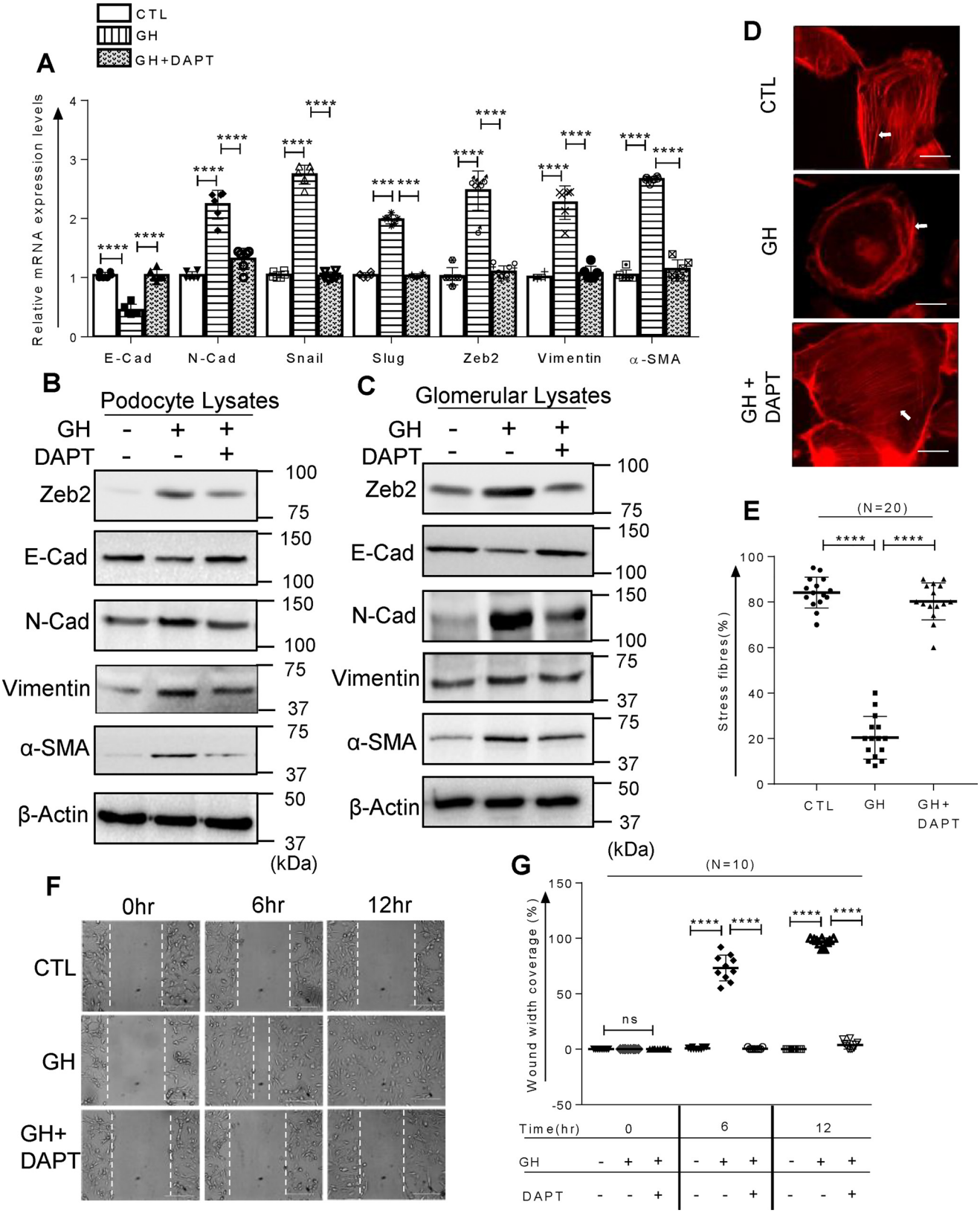

Blocking activated Notch1 signaling abrogates GH-induced proteinuria

Previously, we showed that GH treatment to rodents induces loss of podocyte number (23). GH-treated mice kidney sections were probed for WT1, which specifically express in podocytes. Our data reconfirm that GH treatment results in depletion of podocytes (Fig. 6, *A* and *B*). We also confirmed that GH treatment reduced the physiological functional ability of the kidneys in the mice as analyzed by an increase in urinary albumin-creatinine ratio (UACR) (Fig. 6*C*), and decrease in glomerular filtration rate (GFR) (Fig. 6*D*). We also assessed the extent of proteinuria in GH-treated mice by analyzing the urinary protein content on SDS-PAGE and staining with silver nitrate. GH treatment had increased the amount of protein in urine. Co-treatment of mice with DAPT has rescued the decrease in podocyte number induced by the GH (Fig. 6, *A* and *B*). We also observed that DAPT ameliorated GH-induced UACR (Fig. 6*C*) and GH-induced loss of GFR (Fig. 6*D*). Finally, DAPT also blocked the proteinuria induced by the GH in these mice (Fig. 6*E*). Albumin influx assay (*in vitro*) revealed that DAPT has prevented GH-induced albumin leakage across podocyte monolayer (Fig. 6*F*). Together the data suggest that excess GH impair the podocyte function and induces proteinuria through activated Notch1 signaling.

Notch signaling is hyperactivated in people with diabetic nephropathy

Finally, to confirm the results obtained so far that excess GH induces activated Notch1 signaling in humans, we evaluated the extent of NICD1 expression in people with diabetic nephropathy (DN). As expected, urine from these people showed higher albumin (Fig. S5*A*) and elevated serum creatinine (Fig. S5*B*) levels and decreased glomerular filtration rate (Fig. S5*C*). We observed that there is more urinary protein in these patients as observed by Coomassie Brilliant Blue staining of the urine samples (Fig. 7*A*). Immunohistochemical analysis of the kidney sections from people with diabetes showed increased NICD1, Jag1, and Hes1 expression compared with the healthy controls (Fig. 7*B*). Furthermore, we observed elevated expression of EMT markers α-SMA, N-Cad, and Vimentin in glomerulus in patients with diabetic nephropathy (Fig. 7, *C–F*). All these data confirm that people with diabetic nephropathy have elevated functional Notch signaling in their kidney glomeruli and enhanced expression of EMT markers.

Discussion

In the present article, we show that GH activates Notch1 signaling in podocytes and pharmacological inhibition of γ-secretase blocks the GH-induced EMT induction, infiltration of nonresident cells, fibrosis, GBM thickening, and podocyte foot-process effacement. Glomerular sclerosis and albuminuria are associated with failure of the normal kidney functions. GH induces the albuminuria, whereas the γ-secretase inhibitor treatment under similar conditions kept a constant check on these parameters and thus protects the mice kidneys from fibrosis. More importantly, GH treatment in mice leads to proteinuria, a common symptom associated with diabetic nephropathy, which was successfully abrogated with the γ-secretase inhibitor treatment.

Notch signaling is essential during nephrogenesis, *i.e.* during the embryonic development of glomerular podocytes and proximal tubules (29). On the contrary, Notch signaling is not required for podocyte formation, beyond the stage of the S-shaped body (29, 30). Although, Niranjan *et al.* (14) showed that NICD1 induces apoptosis in rat podocytes, whereas in the experiments performed by Waters *et al.* (15) show that the podocyte-specific expression of NICD1 promoted severe proteinuria and showed evidence of foot-process effacement and progressive glomerulosclerosis. The differences in these two reports can be attributed toward different mice strains used in their studies. Lasagni *et al.* (31) demonstrated that persistent activation of Notch signaling results in mitotic catastrophe and inhibition of the Notch pathway in renal progenitors is prerequisite for the differentiation toward podocyte lineage. Expression of Notch was undetectable in the glomeruli from healthy adult kidneys, whereas a strong up-regulation was observed in podocytes in patients affected by glomerular disorders. Inhibition of Notch signaling in mouse models of focal segmental glomerulosclerosis reduced podocyte loss and improved proteinuria (31). Mice with podocyte-specific deletion of Notch1 were shown to be protected from DN (32). Similarly, podocyte-specific deletion of retinol-binding protein-jk, which is an important downstream component of canonical Notch signaling, has lowered the severity of proteinuria and reduced the podocyte injury in DN rodent model (14). However, the mechanism by which NICD1 is induced during the DN conditions is not yet known. The data presented in our study confirms that excess GH, commonly observed during the DN (33), activates Notch signaling in the podocytes and inhibition of this signaling by γ-secretase inhibitor blocks GH-induced proteinuria and foot-process effacement in mice.

EMT, as well as renal fibrosis, are the shared pathological hallmarks of progressive chronic kidney disease, which comes with diverse etiologies. Hyperglycemia was demonstrated to provoke podocyte EMT through several molecular mechanisms, including activation of Notch signaling (34). Podocyte-specific Notch activation leads to dedifferentiation and its shedding (14, 15). In different models, either treatment with

Figure 4. Activated Notch signaling is required for GH-induced EMT in podocytes. *A*, qRT-PCR analysis showing the expression of EMT markers (E-Cad, N-Cad, Snail, Slug, Zeb2, Vimentin, and α-SMA) in human podocytes treated with GH in the presence or absence of DAPT. β-Actin was used as an internal control. ****, $p < 0.0001$. *B* and *C*, Western blot analysis showing the expression of Zeb2, E-Cad, N-Cad, Vimentin, and α-SMA in (*B*) human podocytes and (*C*) mice glomerular lysates (CTL, GH, and GH + DAPT treatments). *D*, phalloidin staining of podocytes showing F-actin arrangement and changes in stress fibers (indicated by *white arrow*). *E*, phalloidin-stained F-actin stress fibers in podocytes are quantified by ImageJ and data are presented as mean ± S.D. ($n = 20$). ****, $p < 0.0001$. *Scale bars* = 20 μm (×630). *F*, wound healing assay was performed to determine the extent of motility of podocytes from CTL, GH, and GH + DAPT groups and images were captured at the indicated times (0–12 h) using an Olympus inverted microscope (×100) and *scale bar* = 100 μm. *G*, the % area of wound covered by cells was quantified by ImageJ. ****, $p < 0.0001$. Data are presented as mean ± S.D. and statistical significance was analyzed by Student's *t* test. Results shown are representative of three independent experiments.

γ-secretase inhibitors or reducing Notch transcriptional binding protein levels showed a significant amelioration of glomerular injury and fibrosis, demonstrating the role of Notch signaling in podocyte EMT (35, 36). Several upstream master regulators like Wnt and TGF-β etc., are shown to increase the Notch activity (37–39).

Our data indicate that GH induces activated Notch1 signaling in podocytes, and since during DN, GH is up-regulated (20), and we observed increased NICD1 in people with DN, we presume that during DN, GH activates Notch signaling in podocytes. In mice treated with GH, we have shown enhanced glomerulosclerosis and more importantly, DAPT treatment had

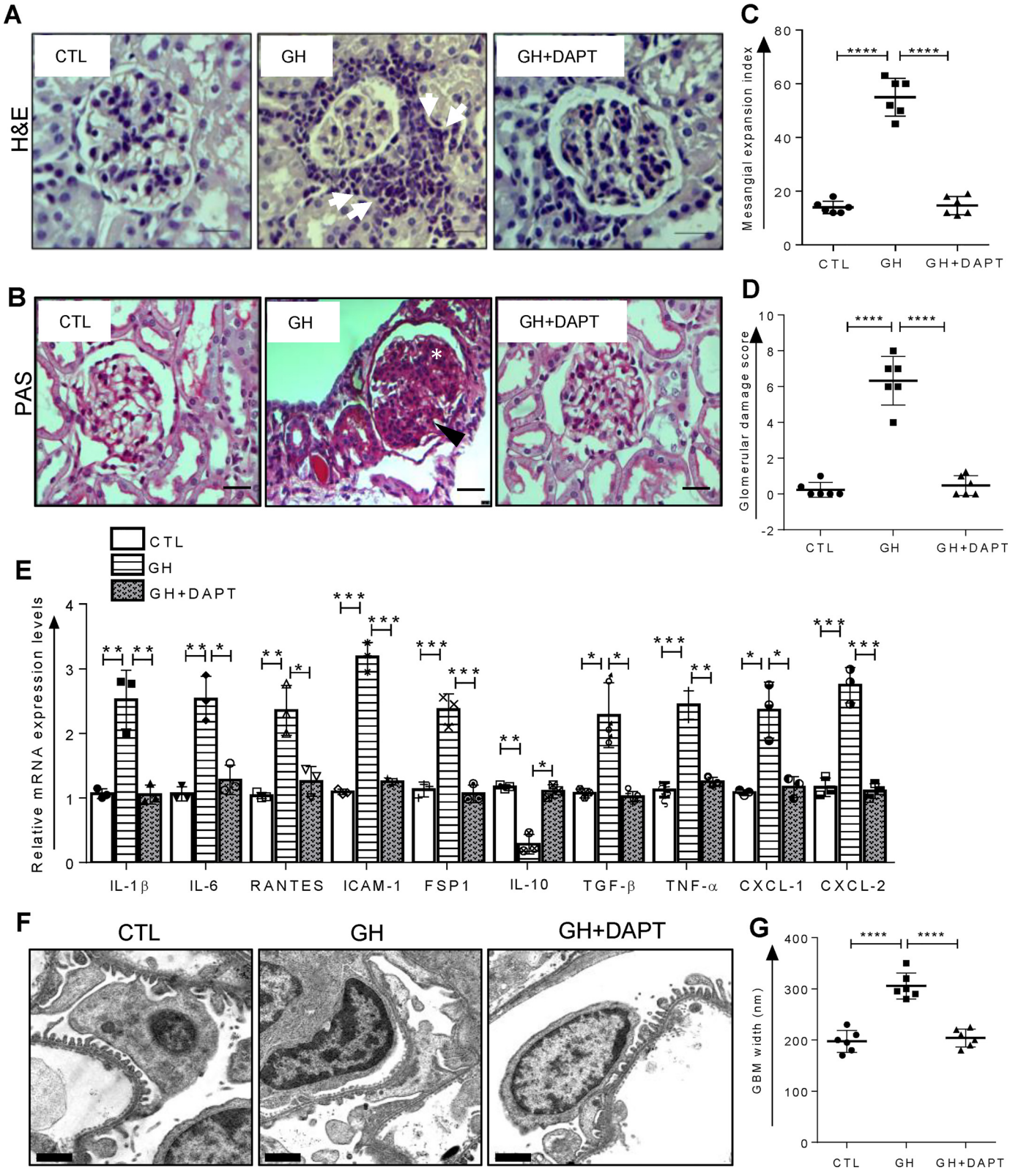

reduced the GH-induced glomerulosclerosis in these mice. Furthermore, our data indicate that activated Notch1 regulates the GH-induced EMT of the podocytes. We had shown previously that GH induces the expression of the EMT transcription factor, ZEB2, which transcriptionally down-regulates P- and E-cadherin expressions in the podocytes (24, 40). In the present article, we show that GH induces NICD1, and treatment of podocytes with γ-secretase inhibitor blocks GH-induced ZEB2 and thus EMT in podocytes.

TGF-β1 is a pro-sclerotic cytokine and it is accepted that TGF-β1 and its downstream SMAD signaling is involved in the development and progression of renal fibrosis in people with DN (41, 42). Studies from our laboratory report that GH regulates the bioavailability of TGF-β1 via regulating the expression of transforming growth factor-β-induced protein (TGFBIp) (23) and induces the expression of Smad-interacting protein, SIP1 (24). Recently, we identified that GH directly stimulates TGF-β expression in podocytes.[4] Whereas DAPT treatment successfully abrogated GH-induced Notch signaling, our data shows that DAPT was not able to reverse GH-induced Jag1 expression. TGF-β1 has been shown to independently regulate Jag1 and Hey1 expression in renal epithelial cells (43, 44). Furthermore, TGF-β–induced EMT can be inhibited by silencing either Hey1 or Jag1 as well as by chemical inactivation of Notch signaling (44). All these data suggest that there is a significant cross-talk between Notch and TGF-β signaling in fine-tuning the EMT phenomenon. How this cross-talk is specifically modulated during GH-depandant podocyte EMT and renal fibrosis needs further studies.

Preclinical studies have shown that DAPT could suppress the Notch signaling and also selective antibodies to preferentially target Notch receptors and ligands have proven successful (44). Based on our data that people with DN show stronger NICD1 staining in the podocytes, as well as blocking NICD1 function through γ-secretase inhibitor abrogates the proteinuria in mice, we believe that proteinuria and glomerulosclerosis in DN can be repressed using γ-secretase inhibitors. However, for the utilization of γ-secretase inhibitors, there are clinical concerns remaining over normal organ homeostasis and significant pathology in multiple organs. Because Notch signaling is not essential for the podocytes after embryonic development, we believe that tissue-specific administration of such inhibitors may offer protection against diabetic nephropathy.

[4] Mukhi D, Nishad R, Singh AK, Mungamuri SK and Pasupulati AK; unpublished data.

Experimental procedures

Reagents

The primary antibodies are as following: anti-activated Notch1 (ab8925), anti-WT-1(ab212951), anti-pSTAT3a (ab76315), anti-t-STAT3a (ab5073), anti-cleaved Notch1 (ab8925), anti-FSP1 (ab41532), and anti-HEY1 (ab154077) were purchased from Abcam (Cambridge, MA). Notch1 Full-length (FL) (number 3608), anti-E-Cadherin (number 3195), anti-N-Cadherin (number 13116), anti-αSMA (number 19245), anti-cleaved Notch1 (number 4147S), anti-ICAM-1 (number 4915), and anti-Actin (number 4970) were purchased from Cell Signaling Technology (Danvers, MA). The anti-HES1 (sc-166410) and anti-ZO-1 (sc-33725) were obtained from Santa Cruz Biotechnology (Dallas, TX). Anti-Vimentin (PAB040Hu01), anti-Col4 (PAA180Hu01), anti-Fibronectin (PAA037Hu01), and anti-JAG1 (PAB807Hu01) were purchased from Cloud-clone (Houston, TX). Anti-ZEB2 (PA5–20980) was purchased from Thermo Fisher Scientific. DAPT (D5942), SIGMAFAST DAB with Metal Enhancer Tablet Set (D0426), phalloidin fluorescein isothiocyanate labeled (P5282), and glutaraldehyde solution (G5882) were obtained from Sigma. Pink pre-stained marker protein (ABIN5662611, Nippon Genetics Europe), Precision Plus Protein Dual Color Standards (Bio-Rad, Hercules, CA), and ProLong™ Diamond Antifade Mountant (P36961) were purchased from Molecular Probes Life Technologies and DyLight 488 and DyLight 564, and Cy5-conjugated secondary antibody were obtained from Vector Laboratories (Burlingame, CA). Primers used in this study procured from Integrated DNA Technologies (Coralville, IA). cDNA reverse transcription kit and SYBR Green Master Mix reagents were obtained from Bio-Rad. All other reagents used were of analytical grade and obtained from Sigma.

Animals and tissues

All the experimental procedures for the animals were pre-approved by the Institutional Animal Ethics Committee of the University of Hyderabad, India. 8-Week-old Swiss Webster male mice weighing nearly 30 ± 5 g were used in this study. The mice were randomly assigned to three groups (6 mice per group): 1) control group (CTL), 2) GH-treated group, and 3) GH + DAPT-treated group. Experimental mice received a single i.p. dose of hGH (1.5 mg/kg/day), whereas control mice have received an equal volume of saline for 4 weeks. The inhibitor groups were received DAPT (10 mg/kg of body weight) per day prior to the GH treatment. After 4 weeks of the experimental period, the mice were placed in individual metabolic cages for collecting 24-h urine to estimate albumin and creatinine. An

Figure 5. Activated Notch signaling is required for GH-induced immune cell infiltration and fibrosis in kidneys. *A*, representative images of H&E staining in glomerular sections from CTL, GH, and GH + DAPT-treated mice. Interstitial infiltration of plasma-lymphocytic cells can be noticed in the GH-treated group (*white arrows*). *Scale bars* indicate 20 μm (×630). *B*, representative images of PAS staining in glomeruli from CTL, GH, and GH + DAPT-treated mice ($n = 6$). *Scale bars* = 20 μm (×630). *C*, mesangial expansion index from PAS-stained images was quantified using ImageJ. Each *dot* represents the average value of 20 glomeruli from a single animal of each group ($n = 6$). ***, $p < 0.004$. *D*, glomerular damage score was derived from PAS-stained images by summing the mesangial expansion (*asterisks*), glomerular capillary blockage, and adhesin of glomerular tuft to Bowman's capsule (*black arrowhead*). Each *dot* represents the average value of 20 glomeruli from a single animal from each group ($n = 6$). ***, $p < 0.004$. *E*, expression of cytokines and chemokines in human podocytes (CTL, GH, and GH + DAPT) was analyzed qRT-PCR. Expression of β-Actin was used as an internal control. *, $p < 0.05$; **, $p < 0.01$; and ***, $p < 0.004$. *F*, TEM images of glomeruli from CTL, GH, and GH + DAPT mice ($n = 6$). Thickening of GBM and effacement of podocyte foot processes was noticed predominantly in GH-treated mice. *Scale bars* indicate 0.5 μm. *G*, thickness of GBM was quantified as described under "Experimental procedures." Data are presented as mean ± S.D. and statistical significance were analyzed by Student's *t* test.

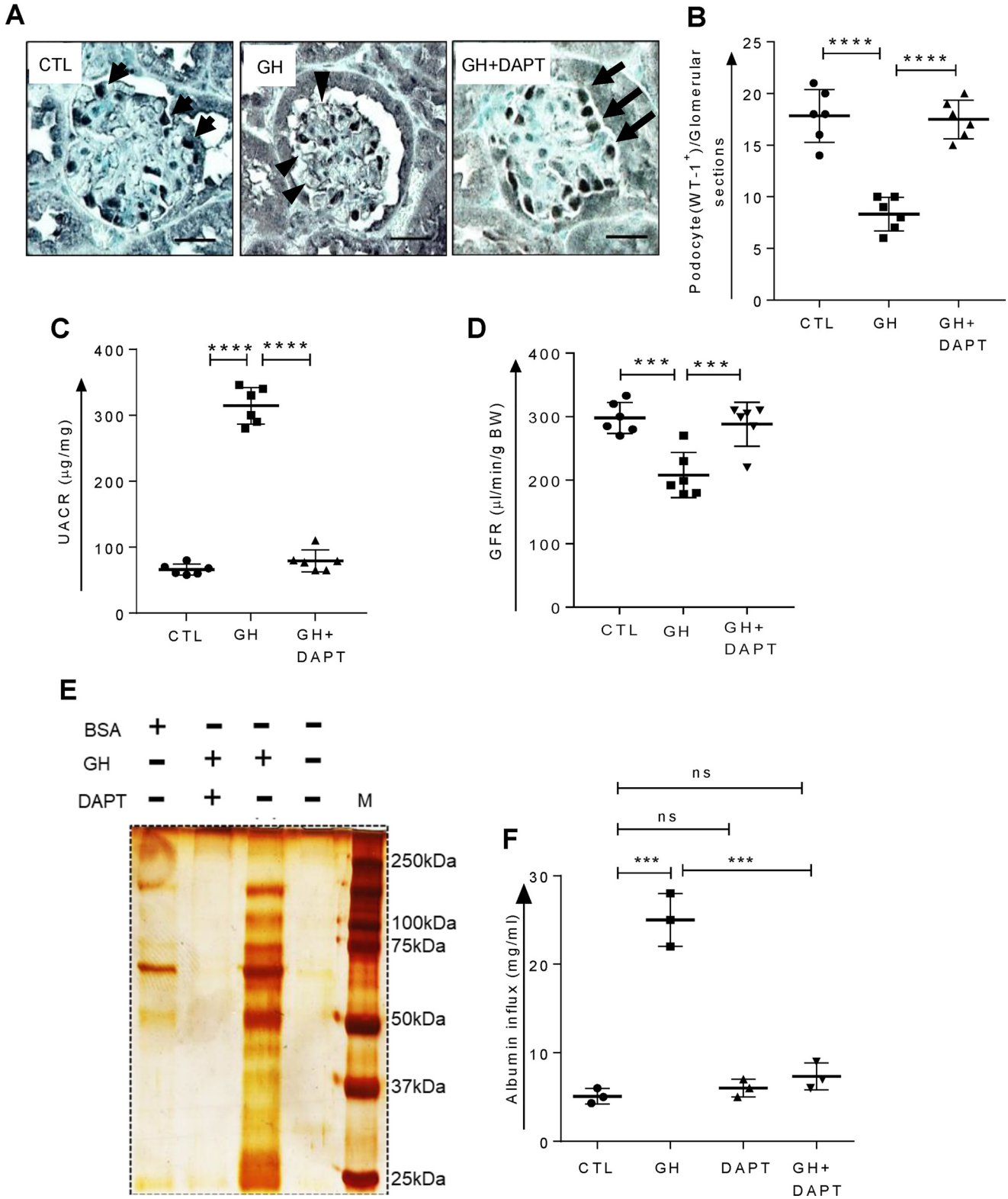

Figure 6. Blockade of Notch signaling protect mice from GH-induced proteinuria. *A*, representative images of immunohistochemical staining for WT1 (podocyte) in glomerulus from CTL, GH, and GH + DAPT-treated mice. *Scale bars* indicate 20 μm. *Arrow* indicates the podocyte and the arrow head indicates loss of podocyte. *B*, average number of $WT1^+$ cells from each mouse from CTL, GH, and GH + DAPT groups. ($n = 6$) **, $p < 0.01$ and ***, $p < 0.004$. We analyzed 20 glomeruli in each mouse for WT^+ cells. *C*, UACR was estimated in CTL, GH, and GH + DAPT-treated mice ($n = 6$). ***, $p < 0.004$; ***, $p < 0.004$. *D*, GFR in CTL, GH, and GH + DAPT-treated mice ($n = 6$). ***, $p < 0.004$. *E*, urinary samples from CTL, GH, and GH + DAPT group mice were subjected to SDS-PAGE and silver stained as described under "Experimental procedures." BSA was used as a standard. *F*, quantification of albumin influx across human podocyte monolayer after 4 h followed by treatment with GH, DAPT, and GH + DAPT for 12 h. ***, $p < 0.004$; *ns*, not significant. Data are presented as mean ± S.D. ($n = 3$) and statistical significance were analyzed by Student's *t* test.

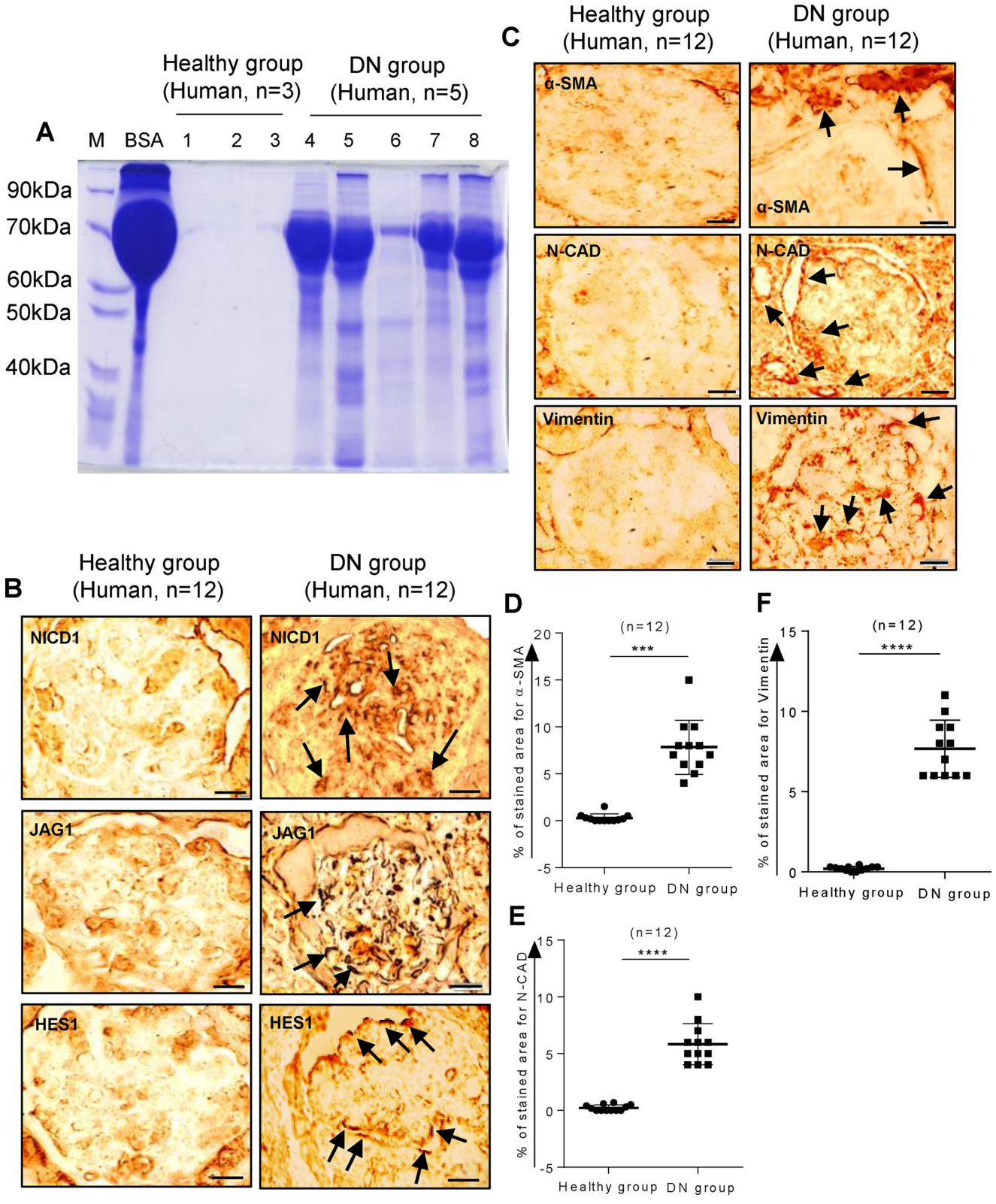

Figure 7. Elevated Notch pathway and EMT in podocytes and proteinuria in people with DN. *A*, urine samples from people with DN ($n = 5$) and healthy volunteers ($n = 3$) were resolved on SDS-PAGE and stained with Coomassie Blue. *B*, representative images of immunohistochemical staining for NICD1, Jag1, and Hes1 in glomerular sections from people with or without DN. *Scale bars* indicate 20 μm (×630). *C*, representative images of immunohistochemical staining for α-SMA, N-Cad, and Vimentin in glomerular sections from people with or without DN. *Scale bars* indicate 20 μm (×630). Quantification of expression of α-SMA (*D*), N-Cad (*E*), and Vimentin (*F*) in 20 glomeruli from each individual with DN compared with people without DN using ImageJ. Data are presented as mean ± S.D. ***, $p < 0.004$ and ****, $p < 0.0001$.

aliquot of urine from mice was subjected to SDS-PAGE gel and silver staining was performed to visualize proteins in the urine (40). We have also estimated GFR in these mice, as described previously (40). We performed immunohistochemistry and Western blotting for analyzing the expression of several markers. For Western blotting, kidneys were collected, and glomeruli were isolated. Protein and RNA were prepared from the glomerular lysate. For histological analysis, kidney cortex was fixed with 4% paraformaldehyde before embedding in paraffin. Paraffin-embedded tissues were sliced longitudinally into 3-μm thick sections, subjected to staining with hematoxylin and eosin, PAS, and Masson's trichrome stainings. Transmission electron microscopic (TEM) images were obtained for glomerular sections from experimental mice groups as described earlier (45).

Human kidney specimens

Kidney specimens were collected without patient identifiers from archived kidney biopsies at Guntur Medical College and Government General Hospital, Andhra Pradesh, India. We selected cases with biopsy-proven diabetic nephropathy and significant proteinuria. The study was approved by the Institutional Review Board of Guntur Medical College and Government General Hospital, Guntur, Andhra Pradesh, India (application number GMC/IEC/120/2018). Our studies abide by the Declaration of Helsinki principles.

Morphological studies

All histological quantifications were evaluated in a blinded manner by two independent investigators. Using kidney sections from these mice ($n = 6$ each group), 20 consecutive glomeruli per mouse were examined for evaluation of glomerular mesangial expansion and an average value of 120 glomeruli from each group presented as a dot plot. The index of the mesangial expansion was defined as the ratio of the mesangial area/glomerular tuft area. The mesangial area was determined by the assessment of the PAS-positive and nucleus-free area in the mesangium using ImageJ (NIH). Ultrastructure of glomerulus was recorded using TEM. For measurement of GBM thickness, we have randomly selected 6 glomeruli per animal ($n = 6$ each group). In each glomerulus, we have selected 6 spots and assessed the thickness of GBM using ImageJ. In the dot plot, each dot represents the average thickness of GBM from a single animal.

Estimation of glomerular filtration rate

GFR in mice was performed at 8 weeks of age using a FIT GFR Test Kit for Inulin according to the manufacturer's instructions (BioPal, Worcester, MA). Briefly, 5 mg/kg of inulin was injected intraperitoneally, followed by serial saphenous bleeds at 30, 60, and 90 min. Next, serum isolation was done and quantified on a inulin ELISA kit. Serum inulin clearance estimation was performed by the nonlinear regression method using a one-phase exponential decay formula ($y = Be - bx$), and GFR was calculated (GFR $= ((I)/(B/b))/KW$, where I is the amount of inulin delivered by the bolus injection, B is y intercept, b is the decay constant, x is time, and KW is kilo weight of the animal). Urinary albumin (number COD11573) and creatinine (number COD11502) levels were estimated using available assay kits (Biosystems, Barcelona, Spain).

Podocyte culture and experimentation

Conditionally immortalized HPC were cultured as described earlier (24). Differentiated podocytes were maintained for 12–16 h in serum-free medium before treating with hGH (Pfizer, NY), pegvisomant (Pfizer), and DAPT (Sigma). Unless otherwise mentioned all the experimental conditions for podocyte cells were given for 12 h. The cell lysate was prepared for RNA isolation or immunoblotting. For immunofluorescence, cells were cultured on coverslips, followed by treatment as mentioned above, subsequent fixation with paraformaldehyde (4%), and blocking with PBS containing normal BSA (5%) before incubation with primary antibodies. The next day, the samples were incubated with Alexa Fluor-conjugated secondary antibodies, and DAPI for 1 h. Images were acquired using a confocal microscope (Zeiss). Albumin influx assay across podocyte monolayer was performed as described earlier (23). Primary podocytes were isolated from mice kidney as described earlier (46).

Immunoblotting

Glomerular lysate from kidney or human podocytes was prepared with lysis buffer (150 mM NaCl, 1% Nonidet P-40, 0.1% SDS, 2 μg/ml of aprotinin, 1 mM PMSF) for 30 min at 4 °C. The homogenate was centrifuged at 12,000 $\times$ g for 25 min at 4 °C and supernatant was collected. An equal amount of protein from different groups was electrophoresed through 10 to 15% SDS-PAGE gel and Western blotting was performed with corresponding primary and secondary antibodies. Blots were developed using the ECL Western blotting substrate (number 1705060, Bio-Rad) and chemiluminescence device (Bio-Rad Versa Doc 5000 MFP).

RNA extraction and qRT-PCR

The total transcripts were extracted by using TRIzol reagent (Invitrogen) and isolated using RNA isolation kit (Qiagen). Next, 1 μg of total RNA was reverse transcribed using the cDNA synthesis kit (Thermo Fisher Scientific). qPCR analysis was performed by the QuantStudio 3 system (Applied Biosystem) with SYBR Green (KAPPABIOSYSTEM, USA) Master Mix using three-step standard cycling conditions with sequence-specific primers. To ensure a single PCR product was amplified, we examined the melting curve for each primer. mRNA expression of each gene was normalized using the expression of β-actin.

Enzyme-linked immunosorbent assay

γ-Secretase activity was quantified by fluorescent microscopy using a γ-secretase activity kit according to the manufacturer's instructions (ImmunoTag, G-Biosciences, St. Louis, MO). Briefly, the γ-secretase activity was determined by quantification of human APH1A (Gamma-Secretase subunit APH-1A) with biotin-conjugated anti-APH1A antibody as a detection antibody. The cleavage-dependent release was measured at 450 nm by using a fluorescent microplate reader (Multiskan GO Microplate Spectrophotometer, Thermo Scientific).

Chemotaxis assay

J774A.1 macrophages were cultured as a monolayer and were scratched using the sterile 10-μl tip and washed with PBS to remove cell debris. Conditioned media from podocytes treated with GH, GH + DAPT, or naive to any treatment was added to J774A.1 macrophage. C5a was used as a positive control with a concentration of 10 ng/ml (47). After the scratch, the images of the wounded area were captured at different time intervals to monitor J774A.1 macrophage migration into the wounded area. The migratory abilities were quantified by measuring the distance between cells in the scratch zone.

F-actin staining

Phalloidin staining for F-actin was performed to visualize the distribution of stress fibers in differentiated podocytes as described previously (48). Briefly, the cells were fixed in 4% paraformaldehyde at room temperature for 15 min after washing, and then permeabilized for 15 min with 0.3% Triton X-100 in PBS followed by 5% BSA blocking. Cells were incubated with rhodamine-phalloidin (Invitrogen Corp.) for 15 min at room temperature to stain F-actin. The slides were examined using confocal laser scanning microscopy. Fifty cells per group were counted to calculate the ratio of cells retaining distinct F-actin fibers. The slides were examined by Leica Microsystems trinocular or Zeiss confocal microscopy.

Wound healing assay

The phenomenon of EMT in podocyte cells was assessed using a wound healing migration assay. A confluent monolayer of podocytes in 6-well plates was wounded with a 10-μl pipette tip following two perpendicular diameters, giving rise to two acellular clear areas per well. After washing with PBS, podocyte cells were treated with GH and GH + DAPT and incubated for 0–12 h and images were captured at different time intervals. The extent of migration of cells to cover wounded area was determined by ImageJ.

Statistical analysis

The data are presented as mean ± S.D. of at least 6 independent experiments unless otherwise mentioned. Prism software (GraphPad Software Inc.) was used to analyze the data. Statistical differences between the groups made using Student's *t* test. Statistical significance was determined as $p < 0.05$.

Author contributions—R. N., D. M., S. V. T., and S. K. M. data curation; R. N., D. M., and S. V. T. methodology; R. N., S. K. M., and A. K. P. writing-original draft; R. N., S. K. M., and A. K. P. writing-review and editing; D. M., S. V. T., S. K. M., and A. K. P. formal analysis; S. K. M. and A. K. P. conceptualization; S. K. M. and A. K. P. supervision; A. K. P. funding acquisition; A. K. P. validation; A. K. P. investigation; A. K. P. visualization; A. K. P. project administration.

Acknowledgment—We acknowledge Prof. Ram K. Menon (University of Michigan, Ann Arbor) for sharing microarray data.

References

1. Nath, K. A. (1992) Tubulointerstitial changes as a major determinant in the progression of renal damage. *Am. J. Kidney Dis.* **20,** 1–17 CrossRef
2. Liu, Y. (2011) Cellular and molecular mechanisms of renal fibrosis. *Nat. Rev. Nephrology* **7,** 684–696 CrossRef Medline
3. Cheng, H. T., Miner, J. H., Lin, M., Tansey, M. G., Roth, K., and Kopan, R. (2003) Gamma-secretase activity is dispensable for mesenchyme-to-epithelium transition but required for podocyte and proximal tubule formation in developing mouse kidney. *Development* **130,** 5031–5042 CrossRef Medline
4. Cheng, H. T., Kim, M., Valerius, M. T., Surendran, K., Schuster-Gossler, K., Gossler, A., McMahon, A. P., and Kopan, R. (2007) Notch2, but not Notch1, is required for proximal fate acquisition in the mammalian nephron. *Development* **134,** 801–811 CrossRef Medline
5. Liu, Z., Chen, S., Boyle, S., Zhu, Y., Zhang, A., Piwnica-Worms, D. R., Ilagan, M. X., and Kopan, R. (2013) The extracellular domain of Notch2 increases its cell-surface abundance and ligand responsiveness during kidney development. *Dev. Cell* **25,** 585–598 CrossRef Medline
6. Chung, E., Deacon, P., and Park, J. S. (2017) Notch is required for the formation of all nephron segments and primes nephron progenitors for differentiation. *Development* **144,** 4530–4539 CrossRef Medline
7. Milano, J., McKay, J., Dagenais, C., Foster-Brown, L., Pognan, F., Gadient, R., Jacobs, R. T., Zacco, A., Greenberg, B., and Ciaccio, P. J. (2004) Modulation of notch processing by γ-secretase inhibitors causes intestinal goblet cell metaplasia and induction of genes known to specify gut secretory lineage differentiation. *Toxicol. Sci.* **82,** 341–358 CrossRef Medline
8. Hayward, P., Kalmar, T., and Arias, A. M. (2008) Wnt/Notch signalling and information processing during development. *Development* **135,** 411–424 CrossRef Medline
9. Zhao, Y., Katzman, R. B., Delmolino, L. M., Bhat, I., Zhang, Y., Gurumurthy, C. B., Germaniuk-Kurowska, A., Reddi, H. V., Solomon, A., Zeng, M. S., Kung, A., Ma, H., Gao, Q., Dimri, G., Stanculescu, A., *et al.* (2007) The notch regulator MAML1 interacts with p53 and functions as a coactivator. *J. Biol. Chem.* **282,** 11969–11981 CrossRef Medline
10. Del Bianco, C., Aster, J. C., and Blacklow, S. C. (2008) Mutational and energetic studies of Notch 1 transcription complexes. *J. Mol. Biol.* **376,** 131–140 CrossRef Medline
11. Liu, Z. J., Xiao, M., Balint, K., Soma, A., Pinnix, C. C., Capobianco, A. J., Velazquez, O. C., and Herlyn, M. (2006) Inhibition of endothelial cell proliferation by Notch1 signaling is mediated by repressing MAPK and PI3K/Akt pathways and requires MAML1. *FASEB J.* **20,** 1009–1011 CrossRef
12. McCright, B. (2003) Notch signaling in kidney development. *Curr. Opin. Nephrol. Hypertens.* **12,** 5–10 CrossRef Medline
13. Vooijs, M., Ong, C. T., Hadland, B., Huppert, S., Liu, Z., Korving, J., van den Born, M., Stappenbeck, T., Wu, Y., Clevers, H., and Kopan, R. (2007) Mapping the consequence of Notch1 proteolysis in vivo with NIP-CRE. *Development* **134,** 535–544 Medline
14. Niranjan, T., Bielesz, B., Gruenwald, A., Ponda, M. P., Kopp, J. B., Thomas, D. B., and Susztak, K. (2008) The Notch pathway in podocytes plays a role in the development of glomerular disease. *Nat. Med.* **14,** 290–298 CrossRef Medline
15. Waters, A. M., Wu, M. Y., Onay, T., Scutaru, J., Liu, J., Lobe, C. G., Quaggin, S. E., and Piscione, T. D. (2008) Ectopic notch activation in developing podocytes causes glomerulosclerosis. *J. Am. Soc. Nephrol.* **19,** 1139–1157 CrossRef Medline
16. Bielesz, B., Sirin, Y., Si, H., Niranjan, T., Gruenwald, A., Ahn, S., Kato, H., Pullman, J., Gessler, M., Haase, V. H., and Susztak, K. (2010) Epithelial Notch signaling regulates interstitial fibrosis development in the kidneys of mice and humans. *J. Clin. Invest.* **120,** 4040–4054 CrossRef Medline
17. Murea, M., Park, J. K., Sharma, S., Kato, H., Gruenwald, A., Niranjan, T., Si, H., Thomas, D. B., Pullman, J. M., Melamed, M. L., and Susztak, K. (2010) Expression of Notch pathway proteins correlates with albuminuria, glomerulosclerosis, and renal function. *Kidney Int.* **78,** 514–522 CrossRef Medline
18. Walsh, D. W., Roxburgh, S. A., McGettigan, P., Berthier, C. C., Higgins, D. G., Kretzler, M., Cohen, C. D., Mezzano, S., Brazil, D. P., and Martin, F. (2008) Co-regulation of Gremlin and Notch signalling in diabetic nephropathy. *Biochim. Biophys. Acta* **1782,** 10–21 CrossRef Medline

19. Niranjan, T., Murea, M., and Susztak, K. (2009) The pathogenic role of Notch activation in podocytes. *Nephron Exp. Nephrol.* **111,** e73–79 CrossRef Medline
20. Pasupulati, A. K., and Menon, R. K. (2019) Growth hormone and chronic kidney disease. *Curr. Opin. Nephrol. Hypertens.* **28,** 10–15 CrossRef Medline
21. Mukhi, D., Nishad, R., Menon, R. K., and Pasupulati, A. K. (2017) Novel actions of growth hormone in podocytes: implications for diabetic nephropathy. *Front. Med.* **4,** 102 CrossRef Medline
22. Kumar, P. A., Brosius F. C., 3rd, Menon, R. K. (2011) The glomerular podocyte as a target of growth hormone action: implications for the pathogenesis of diabetic nephropathy. *Curr. Diabetes Rev.* **7,** 50–55 CrossRef Medline
23. Chitra, P. S., Swathi, T., Sahay, R., Reddy, G. B., Menon, R. K., and Kumar, P. A. (2015) Growth hormone induces transforming growth factor-β-induced protein in podocytes: implications for podocyte depletion and proteinuria. *J. Cell. Biochem.* **116,** 1947–1956 CrossRef Medline
24. Kumar, P. A., Kotlyarevska, K., Dejkhmaron, P., Reddy, G. R., Lu, C., Bhojani, M. S., and Menon, R. K. (2010) Growth hormone (GH)-dependent expression of a natural antisense transcript induces zinc finger E-box-binding homeobox 2 (ZEB2) in the glomerular podocyte: a novel action of GH with implications for the pathogenesis of diabetic nephropathy. *J. Biol. Chem.* **285,** 31148–31156 CrossRef Medline
25. Beel, A. J., and Sanders, C. R. (2008) Substrate specificity of γ-secretase and other intramembrane proteases. *Cell. Mol. Life Sci.* **65,** 1311–1334 CrossRef Medline
26. Haynes, J., Srivastava, J., Madson, N., Wittmann, T., and Barber, D. L. (2011) Dynamic actin remodeling during epithelial-mesenchymal transition depends on increased moesin expression. *Mol. Biol. Cell* **22,** 4750–4764 CrossRef Medline
27. Whitney, J. L., Bilkan, C. M., Sandberg, K., Myers, A. K., and Mulroney, S. E. (2013) Growth hormone exacerbates diabetic renal damage in male but not female rats. *Biol. Sex Differ.* **4,** 12 CrossRef Medline
28. Song, K., Fu, J., Song, J., Herzog, B. H., Bergstrom, K., Kondo, Y., McDaniel, J. M., McGee, S., Silasi-Mansat, R., Lupu, F., Chen, H., Bagavant, H., and Xia, L. (2017) Loss of mucin-type *O*-glycans impairs the integrity of the glomerular filtration barrier in the mouse kidney. *J. Biol. Chem.* **292,** 16491–16497 CrossRef Medline
29. Cheng, H. T., and Kopan, R. (2005) The role of Notch signaling in specification of podocyte and proximal tubules within the developing mouse kidney. *Kidney Int.* **68,** 1951–1952 CrossRef Medline
30. Asanuma, K., Oliva Trejo, J. A., and Tanaka, E. (2017) The role of Notch signaling in kidney podocytes. *Clin. Exp. Nephrol.* **21,** 1–6 CrossRef Medline
31. Lasagni, L., Ballerini, L., Angelotti, M. L., Parente, E., Sagrinati, C., Mazzinghi, B., Peired, A., Ronconi, E., Becherucci, F., Bani, D., Gacci, M., Carini, M., Lazzeri, E., and Romagnani, P. (2010) Notch activation differentially regulates renal progenitors proliferation and differentiation toward the podocyte lineage in glomerular disorders. *Stem Cells (Dayton, OH)* **28,** 1674–1685 CrossRef Medline
32. Sweetwyne, M. T., Gruenwald, A., Niranjan, T., Nishinakamura, R., Strobl, L. J., and Susztak, K. (2015) Notch1 and Notch2 in podocytes play differential roles during diabetic nephropathy development. *Diabetes* **64,** 4099–4111 CrossRef Medline
33. Press, M., Tamborlane, W. V., and Sherwin, R. S. (1984) Importance of raised growth hormone levels in mediating the metabolic derangements of diabetes. *New Engl. J. Med.* **310,** 810–815 CrossRef Medline
34. Ying, Q., and Wu, G. (2017) Molecular mechanisms involved in podocyte EMT and concomitant diabetic kidney diseases: an update. *Ren. Fail.* **39,** 474–483 CrossRef Medline
35. Ahn, S. H., and Susztak, K. (2010) Getting a notch closer to understanding diabetic kidney disease. *Diabetes* **59,** 1865–1867 CrossRef Medline
36. Lin, C. L., Wang, F. S., Hsu, Y. C., Chen, C. N., Tseng, M. J., Saleem, M. A., Chang, P. J., and Wang, J. Y. (2010) Modulation of notch-1 signaling alleviates vascular endothelial growth factor-mediated diabetic nephropathy. *Diabetes* **59,** 1915–1925 CrossRef Medline
37. Wang, Y., and Zhou, B. P. (2011) Epithelial-mesenchymal transition in breast cancer progression and metastasis. *Chin. J. Cancer* **30,** 603–611 CrossRef Medline
38. Collu, G. M., and Brennan, K. (2007) Cooperation between Wnt and Notch signalling in human breast cancer. *Breast Cancer Res.* **9,** 105 CrossRef Medline
39. Leong, K. G., Niessen, K., Kulic, I., Raouf, A., Eaves, C., Pollet, I., and Karsan, A. (2007) Jagged1-mediated Notch activation induces epithelial-to-mesenchymal transition through Slug-induced repression of E-cadherin. *J. Exp. Med.* **204,** 2935–2948 CrossRef Medline
40. Nakuluri, K., Mukhi, D., Nishad, R., Saleem, M. A., Mungamuri, S. K., Menon, R. K., and Pasupulati, A. K. (2019) Hypoxia induces ZEB2 in podocytes: Implications in the pathogenesis of proteinuria. *J. Cell. Physiol.* **234,** 6503–6518 CrossRef Medline
41. Hills, C. E., and Squires, P. E. (2011) The role of TGF-beta and epithelial-to mesenchymal transition in diabetic nephropathy. *Cytokine Growth Factor Rev.* **22,** 131–139 Medline
42. Sutariya, B., Jhonsa, D., and Saraf, M. N. (2016) TGF-β: the connecting link between nephropathy and fibrosis. *Immunopharmacol. Immunotoxicol.* **38,** 39–49 CrossRef Medline
43. Zavadil, J., Cermak, L., Soto-Nieves, N., and Böttinger, E. P. (2004) Integration of TGF-β/Smad and Jagged1/Notch signalling in epithelial-to-mesenchymal transition. *EMBO J.* **23,** 1155–1165 CrossRef Medline
44. Geling, A., Steiner, H., Willem, M., Bally-Cuif, L., and Haass, C. (2002) A gamma-secretase inhibitor blocks Notch signaling *in vivo* and causes a severe neurogenic phenotype in zebrafish. *EMBO Rep.* **3,** 688–694 CrossRef Medline
45. Nakuluri, K., Mukhi, D., Mungamuri, S. K., and Pasupulati, A. K. (2018) Stabilization of hypoxia-inducible factor 1α by cobalt chloride impairs podocyte morphology and slit-diaphragm function. *J. Cell. Biochem.* 10.1002/jcb.28041 CrossRef
46. Katsuya, K., Yaoita, E., Yoshida, Y., Yamamoto, Y., and Yamamoto, T. (2006) An improved method for primary culture of rat podocytes. *Kidney Int.* **69,** 2101–2106 CrossRef Medline
47. Das, D., Barnes, M. A., and Nagy, L. E. (2014) Anaphylatoxin C5a modulates hepatic stellate cell migration. *Fibrogenesis Tissue Repair* **7,** 9 CrossRef Medline
48. Zhou, H., Tian, X., Tufro, A., Moeckel, G., Ishibe, S., and Goodwin, J. (2017) Loss of the podocyte glucocorticoid receptor exacerbates proteinuria after injury. *Sci. Rep.* **7,** 9833 CrossRef Medline